

RSC Advances



This is an *Accepted Manuscript*, which has been through the Royal Society of Chemistry peer review process and has been accepted for publication.

Accepted Manuscripts are published online shortly after acceptance, before technical editing, formatting and proof reading. Using this free service, authors can make their results available to the community, in citable form, before we publish the edited article. This *Accepted Manuscript* will be replaced by the edited, formatted and paginated article as soon as this is available.

You can find more information about *Accepted Manuscripts* in the [Information for Authors](#).

Please note that technical editing may introduce minor changes to the text and/or graphics, which may alter content. The journal's standard [Terms & Conditions](#) and the [Ethical guidelines](#) still apply. In no event shall the Royal Society of Chemistry be held responsible for any errors or omissions in this *Accepted Manuscript* or any consequences arising from the use of any information it contains.

The novel aqueous synthesis methods of ZnTe/ZnSe and Mn²⁺-doped ZnTe/ZnSe Type-II core/shell quantum dots

Yu Song^a, Yang Li^a, Xinyan Wang^b, Xingguang Su^a, and Qiang Ma^{a*}

^a *Department of Analytical Chemistry, College of Chemistry, Jilin University, Changchun, 130012, China*

^b *Changchun Institute of Applied Chemistry Chinese Academy of Sciences, Changchun 230022, China*

*Corresponding author

Tel.: +86-431-85168352

E-mail address: Qma@jlu.edu.cn

Abstract

In this paper, novel approaches for Type-II core/shell quantum dots (ZnTe/ZnSe QDs) and Mn²⁺-doped Type-II core/shell quantum dots (Mn: ZnTe/ZnSe QDs) synthesizing with mercaptopropionic acid (MPA) as stabilizer were proposed. To our knowledge, it is the first time that both core/shell and doping synthesis methods are employed together to prepare photoluminescence Type-II core/shell Mn: ZnTe/ZnSe QDs in aqueous phase. The result showed that PL character of ZnTe/ZnSe QDs significantly changed with the doping of Mn²⁺. And the fluorescence color of QDs can range over an extended emitting wavelength from blue to orange. Also, the increase in PL quantum yield (from 5.3% to 7%) can be obtained. The effects of the experimental conditions for synthesis and the photoluminescence (PL) emission properties were investigated in details. The simple synthetic routes and highlighted good optical properties can make them to be excellent probes for various strategies in chemo/biosensing and bioimaging.

1. Introduction

Semiconductor nanocrystals or quantum dots (QDs) have shown a series of applications in photonic devices and biological probes for fluorescent whole-body imaging,¹⁻³ cancer therapy⁴ and other fields because of their optical and electronic properties including broad absorption, narrow emission spectra, large extinction coefficients, long fluorescence lifetime, resistance to photobleaching and size-tunable emission.⁵⁻⁸ In past decades, considerable research efforts about QDs that produced as fluorescent marker and applied in the biological field have been developed, such as CdE (E=S, Se, Te). But the toxicity of QDs with heavy metal ions was hidden in the field of biomedical pharmacy, medicines and chemical reagents. Many physicochemical properties have been taken to reduce the toxicity of the CdE (E=S, Se, Te) QDs, such as coating them with silica shell or organics.⁹⁻¹⁰ Nevertheless, the efforts cannot entirely be satisfied. In order to meet the needs of avoiding the leakage of heavy metal ions, other type QDs have been reported. Among them, the preparation of Zn-based QDs without heavy metal elements, such as ZnS, ZnSe and ZnTe QDs, is one ideal choice for low-toxicity application. A key problem was that these materials had large band gaps in general was outstanding. As a result, they can hardly emit optical signals in visible ranges, which may severely limit their applicabilities.

Until now, two impactful synthesis routes of available ZnE (E=S, Se, Te) QDs have been reported, including core/shell modification and doping preparation. On the one hand, due to their effective band gap engineering and the tunable optical properties, core/shell heterostructured QDs which were composed of two

semiconductor materials also have attracted much attention. By taking advantage of the type-II band alignment and quantum confinement effects, the type-II core/shell QDs (ZnTe/ZnSe) with strong photoluminescence have been reported.¹¹ In Type-II QDs, the valence and conduction bands in the cores are lower (or higher) in energy than those in the shells and the effective band gap is smaller than that of either the constituent core or shell. In addition, effective band gap of Type-II QDs is governed by the band offsets of the cores and shells.¹²⁻¹⁴ As a result, the Type-II core/shell QDs can emit longer wavelength that is beyond the bulk band gaps of either core or shell. This consequence can be successfully used for vivo imaging and photovoltaic applications.¹⁵⁻¹⁶ So far, many Type-II core/shell systems have been reported, including CdTe/CdSe and CdSe/CdS.¹⁷⁻¹⁸ It has been demonstrated that ZnTe offers an attractive alternative to CdTe as a core material because of the low ionization potential (high valence band edge) for effective holes localization. In recent study, ZnTe/ZnSe QDs has been synthesized as the first cadmium-free Type-II QDs by the organometallic routes.¹⁹⁻²⁰ Bang addressed comprehensive studies on colloidal ZnTe/ZnSe QDs synthetic method. Solution-liquid-solid synthesis of ZnSe/ZnTe quantum wires also has been reported by Buhro and co-workers.²¹ Whereas, the organometallic methods were usually carried out in harsh condition under high temperature which maintained at 200-250 °C. The used organometallic precursors also involved some toxic and expensive reagents, such as trioctylphosphine and tributylphosphine.

On the other hand, QDs doped with transition-metal impurities (e.g. Mn:ZnSe

QDs) has attracted considerable attention as a new generation of luminescent material lately. The most important motivations for incorporation of intentional impurities in these QDs were to improve and control their physical properties such as optical, magnetic, longer fluorescence lifetime and higher thermal stability.²²⁻²³ Doped QDs can potentially retain the distinct advantages of undoped QDs possess, such as narrow and symmetric emission with tunable colors, broad and strong absorption, and reasonable stability. In addition, doped QDs can avoid the self-quenching problem due to their substantial ensemble Stokes shift. Diverse transition-metal and lanthanide ions have been doped into QDs. Mn ions are outstanding in various transition-metal ions for its acceptable toxicity under industrial standards.²⁴ And Mn²⁺-doped ZnSe QDs with good fluorescence properties have been synthesized successfully in aqueous solution.²⁵

In this study, we employed both core/shell and doping synthesis methods to prepare ZnTe/ZnSe QDs (Type-II core/shell QDs) and Mn²⁺-doped ZnTe/ZnSe QDs (Mn:ZnTe/ZnSe QDs) in the aqueous phase. Compared with organometallic routes, aqueous synthesis of hydrophilic QDs shows great promising, which includes biocompatibility, less toxic reagents, lower reaction temperature, comparable PL QY. The optimal precursor ratio and the synthesis conditions for obtaining ZnTe/ZnSe QDs and Mn²⁺-doped ZnTe/ZnSe QDs with good PL emission properties were studied in detail. Compared with ZnSe QDs synthesized in aqueous solution, ZnTe/ZnSe Type-II core/shell QDs and Mn²⁺-doped ZnTe/ZnSe QDs have more reliable optical properties. These results indicated that they had the potential to be applied for

biological assays and imaging investigations as outstanding fluorescent labels.

2. Experimental

2.1 Chemicals

All chemicals were of analytical reagent grade and were used without further purification. Mercaptopropionic acid (MPA) (99%), tellurium powder (~200 mesh, 99.8%), selenium powder (~200 mesh, 99.9%), $\text{Zn}(\text{NO}_3)_2 \cdot 6\text{H}_2\text{O}$ (99.9%), $\text{MnCl}_2 \cdot 4\text{H}_2\text{O}$ (99.9%), and NaBH_4 (99%) were purchased from Aldrich Chemical Co. All chemicals used were of analytical grade. The water used in all experiments had a resistivity higher than $18 \text{ M } \Omega \text{ cm}^{-1}$.

2.2 Synthesis of ZnTe/ZnSe quantum dots

ZnTe/ZnSe QDs were synthesized in aqueous solution as follows: The sodium hydrogen tellurium (NaHTe) and sodium hydrogen selenium (NaHSe) were prepared in aqueous solutions by the reaction of NaBH_4 at first according to the synthesis method of sodium hydrogen telluride.²⁶ The molar ratios of tellurium powder to NaBH_4 and selenium powder to NaBH_4 all were 1:2. 5 mL of $\text{Zn}(\text{NO}_3)_2$ stock solution ($0.5 \times 10^{-2} \text{ M}$) was injected into a 250 mL three-necked flask and degassed for 30 min by bubbling with nitrogen. Fresh NaHTe solution was added to the N_2 -saturated $\text{Zn}(\text{NO}_3)_2$ solution at pH 11 in the presence of MPA as the stabilizing reagent. Zn-to-MPA precursor ratio was 1:6. The pH of the mixture was adjusted to 11 by dropwise addition of a 1M NaOH solution with stirring. The reaction was then switched from nitrogen bubbling to nitrogen flow and subjected to a reflux at $100 \text{ }^\circ\text{C}$ for 1h with a condenser attached. Then we added fresh NaHSe into the three-necked

flask and heated for 4h. Finally, we cooled down the reaction mixture to room temperature and used the as-prepared ZnTe/ZnSe QDs directly without any post-treatments.

2.3 Synthesis of Mn: ZnTe/ZnSe quantum dots

In aqueous solution, Mn: ZnTe/ZnSe QDs were synthesized under different conditions with different adding orders and reaction conditions. In a typical experiment, 0.2 mL MnCl₂ solution (1.25×10^{-2} M), 5 mL of Zn(NO₃)₂ stock solution (0.5×10^{-2} M) and MPA were mixed in a 250 mL three-necked flask and adjusted to pH 11 by addition of a 1 M NaOH solution with stirring. Zn-to-MPA precursor ratio was 1:12. The solution was degassed for 30 min with nitrogen then the freshly prepared NaHTe solution was added into the mixture. The reaction was subjected to a reflux at 100 °C for 1h in nitrogen atmosphere. Afterwards, added fresh NaHSe into the three-necked flask and heated for 6h. After cooling to room temperature, the obtained Mn: ZnTe/ZnSe QDs were used directly without any post-treatments. The QDs solution could be precipitated by ethanol, and the precipitate was centrifuged, washed with ethanol, and dried in vacuum. The obtained powder was used for the next characterization.

2.4 Characterization

Fluorescence measurements were performed on a ShimadzuRF-5301 PC spectrofluorophotometer. UV–Vis absorption spectra were obtained using a GBC Cintra10e UV–Visible spectrometer. In both experiments, a 1 cm path-length quartz cuvette was used. Transmission electron microscopy (TEM) images were obtained

with a Hitachi electron microscope operating at 200 kV. TEM samples were prepared by dropping the aqueous QDs solution onto carbon-coated copper grids and allowing the excess solvent to evaporate. FT-IR spectra were recorded with a Bruker IFS66V FT-IR spectrometer equipped with a DGTS detector (32 scans). Powder X-ray diffraction (XRD) was carried out with a SIEMENS D5005 diffractometer with Cu $K\alpha$ radiation.

3. Results and discussion

3.1 Characterization of ZnTe/ZnSe QDs and Mn: ZnTe/ZnSe QDs

In developed biosensing and bioimaging system, water-soluble QDs are highly required for their ligand exchange with bifunctional small molecules. To make the QDs water-soluble, we chose MPA as small molecules stabilizer to accomplish QDs decoration. Water-soluble ZnTe/ZnSe QDs and Mn: ZnTe/ZnSe QDs with MPA as capping reagent in this study were prepared directly in aqueous solutions. We studied their PL properties by the comparison spectra for the emission intensities of QDs which were shown in **Fig. 1**. The emission peak of ZnTe/ZnSe QDs was at 480nm (**Fig. 1 b**). It was different from ZnSe QDs emission peak at 445nm (**Fig. 1 a**) obviously. Moreover, a red-shift about 100nm of the band-edge emission features can be observed with the Mn^{2+} doping to the ZnTe/ZnSe QDs (**Fig. 1 c**). This transformation can be counted as a signature of distinct feature to indicate that the incorporation of Mn^{2+} into the ZnTe/ZnSe QDs was successful. **Fig. 1** also showed a photograph of the ZnSe QDs, ZnTe/ZnSe QDs and Mn: ZnTe/ZnSe QDs under UV light, severally. From the photograph, we can see that under UV light ZnTe/ZnSe QDs

and Mn: ZnTe/ZnSe QDs in aqueous solution emitted strong blue and yellow fluorescence, respectively. It was corresponding to the fluorescence emission spectra showed.

FT-IR spectra of the purified and dried ZnTe/ZnSe QDs and Mn: ZnTe/ZnSe QDs with MPA as capping reagent were given in **Fig. 2**. The most pronounced IR absorption bands of ZnTe/ZnSe QDs and Mn: ZnTe/ZnSe QDs occurred at 3413.14 cm^{-1} (**Fig. 2a**) O-H stretching vibration and 3403.91 cm^{-1} (**Fig. 2b**) O-H stretching vibration. The symmetric and asymmetric stretching vibrations of the carboxylate groups appeared (**Fig. 2a** 1577.56 cm^{-1} (svCOO⁻) and 1403.14 cm^{-1} (mvCOO⁻), **Fig. 2b** 1577.56 cm^{-1} (svCOO⁻) and 1405.06 cm^{-1} (mvCOO⁻)). The spectrum of ZnTe/ZnSe QDs and Mn: ZnTe/ZnSe QDs also displayed the bands assigned to the 2925.62 cm^{-1} (νCH_2), 990.34 cm^{-1} (δOH) in **Fig. 2a** and the 2921.77 cm^{-1} (νCH_2), 991.28 cm^{-1} (δOH) in **Fig. 2b**. But the vibration peak of S-H (2550–2670 cm^{-1} , $\nu\text{S-H}$) which should exist in MPA was not present in the FT-IR spectra. This resulted from the covalent bonds between thiols and Zn atoms on the surface of QDs. It indicated that the ZnTe/ZnSe QDs and Mn: ZnTe/ZnSe QDs have been capped by the stabilizer MPA.

3.2 Optimization for the synthesis of ZnTe/ZnSe QDs

In the synthesis process, nucleation of host formed after the addition of precursors NaHTe and Zn firstly. The host nucleation ZnTe was without emission growth. Considering the solubility and reactivity of Se powder under basic conditions, NaBH_4 was used to assist the dissolution of Se powder at room temperature. Then

ZnSe shell formed following by the introduction of Se precursor NaHSe. **Fig. 3** showed the wide-angle X-ray diffraction (XRD) patterns (**Fig. 3A**) and TEM images (**Fig. 3B**) of undoped ZnTe/ZnSe QDs powder sample. And Selected area electron diffraction (SAED) patterns are recorded as shown in the inset of panel A of **Fig. 3**. It showed micrograph of about 4-5 nm diameter ZnTe/ZnSe QDs. Bars on the top and bottom of **Fig. 3A** represented bulk cubic structures of ZnSe and ZnTe, respectively. The XRD pattern of the QDs exhibited characteristic peaks at ca. 27.5, 46.5, and 53.4° corresponding to the (111), (220) and (311) reflecting planes of cubic zinc blende. Additionally, the main strong peaks were observed are for (111), which clearly matches for both ZnTe and ZnSe bulk material that belonged to cubic phase structure. The crystal structure demonstrated by XRD diffractogram in the sample was zinc blende. It was in accord with the structure that Bang and Park reported.²⁰

According to previous study, the ZnTe core-only structures showed no PL. It was presumably due to the unstable surfaces which are the prone to nonradiative traps. While the ZnSe that deposited as shell material can passivate the trap sites of ZnTe core QDs. This could go a step further to make the ZnTe/ZnSe QDs become emissive.²⁰ The Se-to-Te ratio would play an important role in the PL emission of ZnTe/ZnSe QDs during the reaction process. **Fig. 4** showed the changes in PL intensity for a series of ZnTe/ZnSe QDs of different Se-to-Te ratio. When it changed between 5:1 and 20:1, the PL intensity increased markedly with the Se-to-Te ratio increased. With the amount of Se increasing, the shell grew thicker. At the ratio of 20:1, PL intensity reached its maximum value. A 9-fold increase in PL intensity can be obtained.

However, the much thicker ZnSe shells can enhance Type-II spatial separations between electrons and holes, which resulted the PL intensity decreased (**Fig. 4c**).²⁷⁻²⁹ As a result, the brightest sample among the series studies was the one that Se-to-Te ratio was 20:1.

As **Fig. 5A** shown, the PL emission spectrum of ZnTe/ZnSe QDs with 350 nm excitation showed the emission peaks at about 480 nm in various pH conditions which were different from the emission peak of ZnSe QDs (445 nm). It indicated that the ZnTe/ZnSe QDs have been synthesized successfully. The pH below 5.9 was unsuitable for the synthesis of ZnTe QDs. Only in weak acidic and alkalic matrix, ZnTe QDs can be successfully prepared.³⁰ Besides, the usual synthetic condition of ZnSe was alkaline according to former article reported.²⁰ The PL intensity of QDs was quenched in acid circumstance such as pH=6 (**Fig. 5A a**). The PL intensity of pH 6 was similar to that of pH 7 (**Fig. 5A b**). The reason was that low pH surrounding was not in favor of ZnSe shell deposition. In addition, a portion of ZnTe QDs with a thin ZnSe shell deposition oxidized to insoluble Te powder when they were exposed to air. With pH of solution increased to alkalinity, the PL became enhanced. It can reach to 6-8 fold compared with the PL intensity in pH 7 solution. According to a series of experiments, the pH 11 alkalinity solution was chosen as the optimum synthetic pH condition for ZnTe/ZnSe QDs. The influence of heating time was also studied, and the results were shown in **Fig. 5B**. The time was varied from 1h to 4h. With increasing in heating time, the deposition of ZnSe shell was in progress. At the beginning of the reaction, the PL intensity of small size QDs was weak. With the

heating time increasing, the nanocrystal grew and PL intensity sharply increased to 91.9% in 3 hour, substantially. And the PL intensity reached the maximum at 3.5 h after the addition of NaHSe. From 3.5 h to 4 h, the PL intensity became stable with only 2% increment. Therefore, 3.5 h was selected as the optimum synthetic time. The final quantum yield (QY) of the ZnTe/ZnSe QDs was 5.3%. It can be competitive with organometallic route whose QY was 6%.²⁰

3.3 Optimization for the synthesis of Mn: ZnTe/ZnSe QDs

Since doped QDs have been put forward, they attracted much attention immediately. The main reason was that both electronic states and electromagnetic fields were modified and the optical properties of impurities may change consumedly. In order to improve the wavelength properties of ZnTe/ZnSe QDs, we doped metal ions with ZnTe/ZnSe QDs. We chose Mn^{2+} as dopant for ZnTe/ZnSe QDs because of its acceptable toxicity and well possibility of altering and controlling QDs physical properties. The dopant Mn^{2+} led to some interesting results such as emission red-shift and the PL stabilization. Mn^{2+} doped QDs exhibited a typical photoluminescence. The pure and strong dopant emission was observed at about 575 nm due to the $\text{Mn}^{2+} \ ^4\text{T}_1 \rightarrow \ ^6\text{A}_1$ transition. These phenomena were not found in the bulk state because their electronic states were confined in a very small volume. In comparison to the absorption band gap of the ZnTe/ZnSe QDs, Mn^{2+} doped QDs had a large Stokes shift resulted from their relatively small emission energy gap. Mn^{2+} doped ZnTe/ZnSe QDs with substantial ensemble Stokes shift can avoid the self-quenching problem that usually owned to intramolecular ground-state dimer complex or energy transfer

between adjacent QDs. Additionally, as a dopant, a amount of Mn^{2+} would diffuse into the host layer during the annealing process in the synthesis. The ions in each individual d-dot are clustered together in close proximity.³¹ The emission centers away from the surface trap states of the nanocrystals, and thereby improved the optical performance of the nanocrystals. So the Mn ions in the ZnTe/ZnSe QDs host crystal field could increase the PL intensity.

There are three strategies with different precursors adding orders according to Peng and Yan reported.³² Following the different orders, several different PL spectra of QDs were exhibited in **Fig. 6**. The insert showed the synthesis process. The first strategy (**Fig. 6a**) was formed ZnTe before adding Mn^{2+} . This growth-doping was forming the nuclei with pure dopant cations with following by the growth of a host shell on the core. After dopant growth, on the surface-doped nucleus coated a new layer of shell. The PL intensity of QDs increased slowly upon heating at 100 °C and reached its maximum value (PL QY = 1%) after 5 h. The maximum value was so weak that cannot reach the satisfactory degree. The second strategy (**Fig. 6b**) was introducing both dopant and host ions into the reaction system at the same time. After heated for 5h, the spectrum of QDs had two peaks at 483 nm and 566 nm, respectively. The intensities of them were similar. It may result from a part of undoped ZnTe/ZnSe QDs and surface-adsorbed dopants which were often mixed with the doped QDs. What is more, the peak at 483 nm was stronger than the one at 566 nm in some extent that would influence the PL intensity measurement for Mn: ZnTe/ZnSe QDs. It indicated that the doping efficiency which also related to the types of Mn^{2+} precursor

and particle size was low. The PL QY was 1.5%. For these reasons, this strategy was not appropriate. In the last strategy (**Fig. 6c**), Mn^{2+} and NaHTe were mixed at the beginning. Then added the Zn^{2+} and NaHSe were successively. The Mn^{2+} -doped ZnTe/ZnSe QDs were prepared through a nucleation-doping strategy which was realized by mixing dopant and host precursor during nucleation. Mn^{2+} can be well doped in host during this process. As a result, MnTe was formed. After nucleation, the reaction condition was tuned to a sufficient mild degree, which induced the inactivation of the precursors. Then the growth of the ZnSe shell became the main process. Besides a number of ZnSe deposited on the core as shell, some excess also remained in solution as the formation of ZnTe/ZnSe with an observable fluorescence signal (EM 475 nm). So the production had two emissions at 475nm and 570nm, respectively. The intensity of peak at 475 nm was lower than the one at 570 nm in a large extent. This result indicated that in the process of nucleation-doping strategy most core/shell QDs was the doped successfully. Also the PL intensity at 570 nm was 9-fold to the production of growth-doping under the same reaction condition. Compared with the other two synthetic approaches, the PL intensity of the last strategy was the strongest in the same condition. The reason was that the nucleation-doping cannot be quenched by lowering the temperature.³³⁻³⁶ According to the result, we chose the last synthesis method for Mn: ZnTe/ZnSe QDs synthesis.

In later optimization conditions experiments, the concentrations of the dopant Mn^{2+} in the nuclei was tuned by varying the precursor ratio Zn-to-Mn from 3% to 10%. Just as **Fig. 7A** shown, PL intensity changed with Zn-to-Mn ratio and reached to

maximum at 5%. Compared with 5%, higher Zn-to-Mn ratio which represented fewer Mn^{2+} ions doped into the ZnTe/ZnSe QDs can cause PL intensity quenched. This phenomenon provided the evidence that the doping concentration of Mn^{2+} ions decreased when the Zn-to-Mn ratio increased higher. However, too much Mn^{2+} ions was also not satisfactory to PL intensity. It could be clarified by the effect of MnTe nuclei. When Zn-to-Mn ratio was lower than 5%, the PL intensity was decreased with ratio decreased. The reason was that larger nuclei formed during the nucleation–doping process which was not as uniform as smaller ones.²³ It also can be seen that the influence of emission at 475 nm weakened by adjusting Zn-to-Mn ratio and reached to 32% of 570 nm. So the optimum Zn-to-Mn ratio was 5%. **Fig. 7B** showed the influence of heating time. PL intensity exhibited the steadily increasing trend with increasing refluxing time and reached the maximum until 6 h. It was consistent with the growth of the ZnSe shell. However, the PL intensity of Mn^{2+} -doped ZnTe/ZnSe QDs increasing trend reversed for longer heating time after 6 h. The reason may be the effect of Ostwald ripening. In this process, larger nanocrystals have been formed of at the expense of smaller ones. So the PL intensity quenched. The best quantum yield (QY) of the Mn: ZnTe/ZnSe QDs was obtained at 7%. The QY was higher than Mn: ZnSe whose QY was 2.4% and similar to the core/shell ZnSe:Mn/ZnS QDs with a PL QY about 9% in water.^{25,37}

3.4 The stability of ZnTe/ZnSe QDs and Mn: ZnTe/ZnSe QDs

In order to test the potential application value of ZnTe/ZnSe QDs and Mn: ZnTe/ZnSe QDs, we compared the optical stability of them. The PL emission intensity

of Mn^{2+} (${}^4\text{T}_1 \rightarrow {}^6\text{A}_1$) doped ZnTe/ZnSe QDs remained well intensity under room temperature and daylight in a week (**Fig. 8**). While the ZnTe/ZnSe QDs PL intensity decreased after two days and remained only about 15% after a week. This result demonstrated that the PL stability of Mn: ZnTe/ZnSe QDs was much better than that of ZnTe/ZnSe QDs in the air. It may be the result of the unique structure of Mn: ZnTe/ZnSe QDs. After doping with Mn^{2+} by the nucleation–doping method, the host was overcoated by ZnSe shell which can protect the nucleus with the dopant. So the stability has been improved largely. Although the stability of ZnTe/ZnSe QDs was not as good as Mn: ZnTe/ZnSe QDs, the successful aqueous synthesis of low-toxic ZnTe/ZnSe QDs provided a new way for the nanometer materials synthesis which can be used for the detection. For the potential application of Mn: ZnTe/ZnSe QDs in biosensing and bioimaging, the stability in the phosphate (2 mmol/L), TRIS (10 mmol/L) and borate (0.2 mol/L) buffered saline system also has been investigated, respectively. A sequence pH of different buffer solution was mixed with QDs under the volume ratio of 1:1 (as shown in **Fig. 9**). There was no obvious quenching in any buffer solution. The good stability, low toxicity and water solubility were helpful to apply Mn: ZnTe/ZnSe QDs in biomedical assays and imaging of cells tissues, even in vivo investigations.

4 Conclusions

In summary, the aqueous synthesis of MPA capped ZnTe/ZnSe Type-II core/shell QDs was successfully carried out by a facile route. In order to improve the emission and stability of ZnTe/ZnSe QDs, Mn^{2+} -doped ZnTe/ZnSe QDs were obtained through

nucleation–doping strategy in aqueous solution for the first time. Much more efforts have been made to explore the properties, optimization of synthesis as well as luminescence performances of ZnTe/ZnSe QDs and Mn: ZnTe/ZnSe QDs. The obtained QDs showed extremely water soluble and photostable. Moreover, they all had lower toxicity than the traditional QDs in aqueous solution. Due to their unique and stable optical properties, the non-cadmium ZnTe/ZnSe QDs and Mn: ZnTe/ZnSe QDs can be used in the areas of biomedical applications as a novel type of fluorescent nanoprobe.

Notes and references

- 1 X. Michalet, F. F. Pinaud, L. A. Bentolila, J. M. Tsay, S. Doose, J. J. Li, G. Sundaresan, A. M. Wu, S. S. Gambhir and S. Weiss, *Science*, 2005, **307**, 538-544.
- 2 X. Gao, Y. Cui, R. M. Levenson, L. W. K. Chung, S. Nie, *Nat. Biotechnol.*, 2004, **22**, 969-976.
- 3 W. Cai, D. W. Shin, K. Chen, O. Gheysens, Q. Cao, S. X. Wang, S. S. Gambhir and X. Chen, *Nano Lett.*, 2006, **6**, 669-676.
- 4 L. X. Shi, B. Hernandez and M. Selke, *J. Am. Chem. Soc.*, 2006, **128**, 6278-6279.
- 5 S. A. Empedocles and M. G. Bawendi, *Science*, 1997, **278**, 2114-2117.
- 6 A. P. Alivisatos, *Science*, 1996, **271**, 933-937.
- 7 S. Coe, W. K. Woo, M. Bawendi and V. Bulovic, *Nature*, 2002, **420**, 800-803.
- 8 J. Lim, S. Jun, E. Jang, H. Baik, H. Kim and J. Cho, *Adv. Mater.*, 2007, **19**, 1927-1932.
- 9 S. T. Selvan, T. T. Tan and J. Y. Ying, *Adv. Mater.*, 2005, **17**, 1620-1625.

- 10 J. Lovric, S. J. Cho, F. M. Winnik and D. Maysinger, *Chem. Biol.*, 2005, **12**, 1227-1234.
- 11 Q. Zhang, A. Shen, I. L. Kuskovsky and M. C. Tamargo, *J. Appl. Phys.*, 2011, **110**, 034302
- 12 S. Kim, B. Fisher, H. J. Eisler and M. G. Bawendi, *J. Am. Chem. Soc.*, 2003, **125**, 11466-11467.
- 13 C. Y. Chen, C. T. Cheng, C. W. Lai, Y. H. Hu, P. T. Chou, Y. H. Chou and H. T. Chiu, *Small*, 2005, **1**, 1215-1220.
- 14 D. Dorfs, A. Salant, I. Popov and U. Banin, *Small*, 2008, **4**, 1319-1323.
- 15 S. Kim,; Y. T. Lim,; E. G. Soltesz,; A. M. De Grand,; J. Lee,; A. Nakayama,; J. A. Parker,; T. Mihaljevic,; R. G. Laurence,; D. M. Dor,; L. H. Cohn,; M. G. Bawendi and J. V. Frangioni, *Nat. Biotechnol.*, 2004, **22**, 93-97.
- 16 H. Zhong, Y. Zhou, Y. Yang, C. Yang and Y. Li, *J. Phys. Chem. C*, 2007, **111**, 6538-6543.
- 17 K. Yu, B. Zaman, S. Romanova, D. S. Wang and J. A. Ripmeester, *Small*, 2005, **1**, 332-338.
- 18 X. G. Peng, M. C. Schlamp, A. V. Kadavanich and A. P. Alivisatos, *J. Am. Chem. Soc.*, 1997, **119**, 7019-7029.
- 19 S. M. Fairclough, E. J. Tyrrell, D. M. Graham, P. J. B. Lunt, S. J. O. Hardman, A. Pietzsch, F. Hennes, J. Moghal, W. R. Flavell, A. A. R. Watt and J. M. Smith, *J. Phys. Chem. C*, 2012, **116**, 26898-26907.
- 20 J. Bang, J. Park, J. H. Lee, N. Won, J. Nam, J. Lim, B. Y. Chang, H. J. Lee, B.

- Chon, J. Shin, J. B. Park, J. H. Choi, K. Cho, S. M. Park, T. Joo and S. Kim, *Chem. Mater.*, 2010, **22**, 233-240.
- 21 Dong, A.; Wang, F.; Daulton, T. L.; Buhro, W. E., *Nano Lett.*, 2007, **7**, 1308-1313.
- 22 N. Pradhan, D. Goorskey, J. Thessing and X. G. Peng, *J. Am. Chem. Soc.*, 2005, **127**, 17586-17587.
- 23 N. Pradhan and X. G. Peng, *J. Am. Chem. Soc.*, 2007, **129**, 3339-3347.
- 24 X. Peng, *Nano. Res.*, 2009, **2**, 425-447.
- 25 C. Wang, X. Gao, Q. Ma and X. G. Su, *J. Mater. Chem.*, 2009, **19**, 7016-7022.
- 26 H. Zhang, L. P. Wang, H. M. Xiong, L. H. Hu, B. Yang and W. Li, *Adv. Mater.*, 2003, **15**, 1712-1715.
- 27 L. J. Zu, A. W. Wills, T. A. Kennedy, E. R. Glaser and D. J. Norris, *J. Phys. Chem. C*, 2010, **114**, 21969-21975.
- 28 S. Kim, B. Fisher, H. J. Eisler and M. G. Bawendi, *J. Am. Chem. Soc.*, 2003, **125**, 11466-11467.
- 29 D. Dorfs, A. Salant, I. Popov and U. Banin, *Small*, 2008, **4**, 1319-1323.
- 30 S. H. Xu, C. L. Wang, Q. Y. Xu, H. S. Zhang, R. Q. Li, H. B. Shao, W. Lei and Y. P. Cui, *Chem. Mater.*, 2010, **22**, 5838-5844.
- 31 Y. P. Zhang, C. L. Gan, J. Muhammad, D. Battaglia, X. G. Peng, and M. Xiao, *J. Phys. Chem. C*, 2008, **112**, 20200-20205.
- 32 P. Wu and X. P. Yan, *Chem. Soc. Rev.*, 2013, **42**, 5489-5521.
- 33 Y. A. Yang, O. Chen, A. Angerhofer and Y. C. Cao, *J. Am. Chem. Soc.*, 2006, **128**, 12428-12429.

- 34 Y. A. Yang, O. Chen, A. Angerhofer and Y. C. Cao, *J. Am. Chem. Soc.*, 2008, **130**, 15649-15661.
- 35 Y. A. Yang, O. Chen, A. Angerhofer and Y. C. Cao, *Chem.–Eur. J.*, 2009, **15**, 3186-3197.
- 36 B. B. Srivastava, S. Jana, N. S. Karan, S. Paria, N. R. Jana, D. D. Sarma and N. Pradhan, *J. Phys. Chem. Lett.*, 2010, **1**, 1454-1458.
- 37 A. Aboulaich, M. Geszke, L. Balan, J. Ghanbaja, G. Medjahdi, and R. Schneider, *Inorg. Chem.*, 2010, **49**, 10940–10948.

Caption of figure

Fig. 1 A: The fluorescence spectra of (a) ZnSe QDs, (b) ZnTe/ZnSe QDs and (c) Mn:ZnTe/ZnSe QDs. The inset shows a photograph of (a) ZnSe QDs, (b) ZnTe/ZnSe QDs and (c) Mn: ZnTe/ZnSe QDs under UV light.

Fig. 2 FT-IR spectrum of (a) ZnTe/ZnSe QDs and (b) Mn:ZnTe/ZnSe QD.

Fig. 3 (A) XRD pattern and (B) TEM images of ZnTe/ZnSe QDs. Inset: Selected

electron diffraction pattern of the corresponding particles

Fig. 4 The fluorescence spectra of ZnSe/ZnSe QDs with different ratios of Se-to-Te (a) 5:1 (b) 10:1 (c) 30:1 (d) 20:1.

Fig. 5 (A) The influence of pH on the PL intensity of ZnTe/ZnSe QDs (a) pH 6 (b) pH 7 (c) pH 9 (d) pH 10. Inset: A plot of normalized intensity against the pH. (B) The influence of heating time on the PL intensity of ZnTe/ZnSe QDs (a) 1.5 h (b) 2 h (c) 2.5 h (d) 3 h (e) 3.5 h (f) 4 h. Inset: A plot of normalized intensity against the heating time.

Fig. 6 The fluorescence spectra of Mn:ZnTe/ZnSe QDs with different synthesis methods (a) Dopant Mn^{2+} introduction after ZnTe nucleation (growth doping) (b) Dopant Mn^{2+} introduction along with host precursors Zn^{2+} and NaHTe (c) Dopant Mn^{2+} introduction before nucleation of ZnTe (nucleation doping). Inset: The schematic illustration of (a) (b) and (c)

Fig. 7 The fluorescence spectra of ZnTe/ZnSe QDs with (A) different ratios of Mn-to-Zn (a) 10% (b) 3% (c) 8% (d) 5% and (B) different heating time (a) 1 h (b) 2 h (c) 3 h (d) 7 h (e) 4 h (f) 6 h.

Fig. 8 Stability of ZnTe/ZnSe QDs and Mn: ZnTe/ZnSe QDs in daylight.

Fig. 9 Stability of Mn: ZnTe/ZnSe QDs in phosphate, TRIS and borate buffered saline system. I_0 represented the original PL intensity of QDs, I represented the PL intensity of QDs-buffer solution after 30 min.

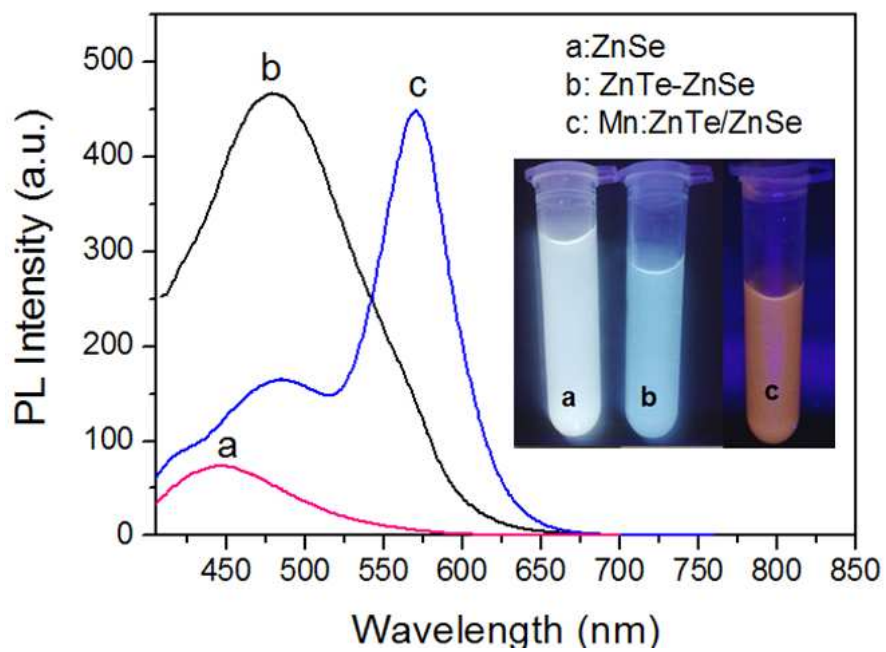


Fig. 1 A: The fluorescence spectra of (a) ZnSe QDs, (b) ZnTe/ZnSe QDs and (c) Mn:ZnTe/ZnSe QDs. The inset shows a photograph of (a) ZnSe QDs, (b) ZnTe/ZnSe QDs and (c) Mn: ZnTe/ZnSe QDs under UV light.

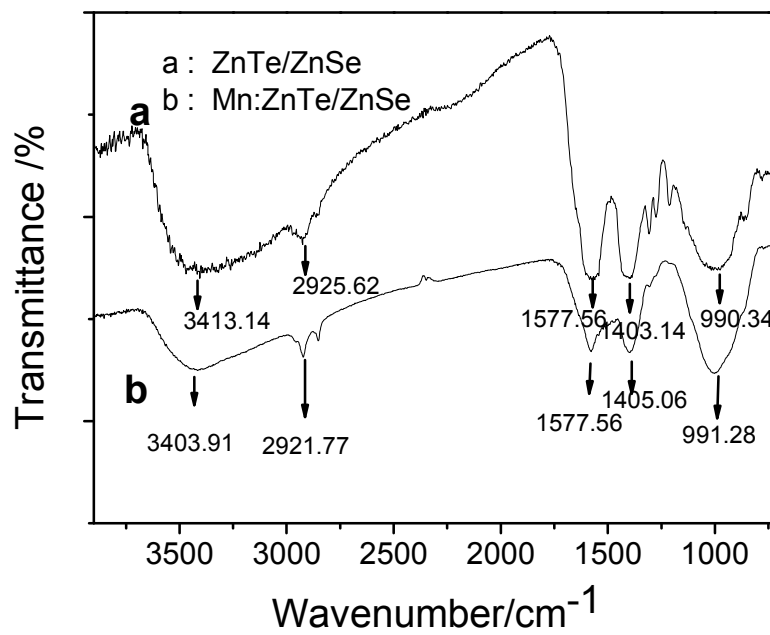


Fig. 2 FT-IR spectrum of (a) ZnTe/ZnSe QDs and (b) Mn:ZnTe/ZnSe QD.

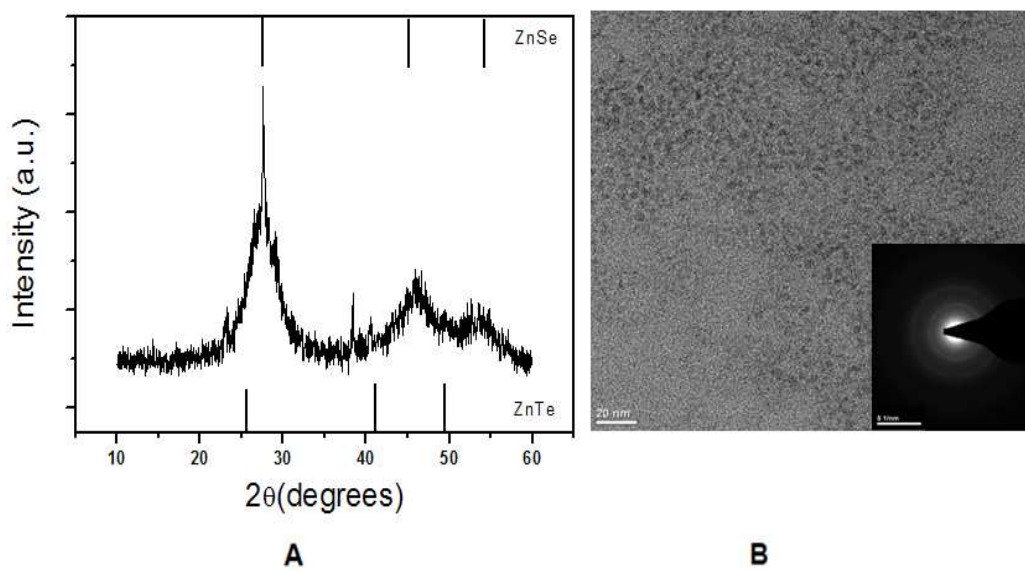


Fig. 3 (A) XRD pattern and (B) TEM images of ZnTe/ZnSe QDs. Inset: Selected electron diffraction pattern of the corresponding particles

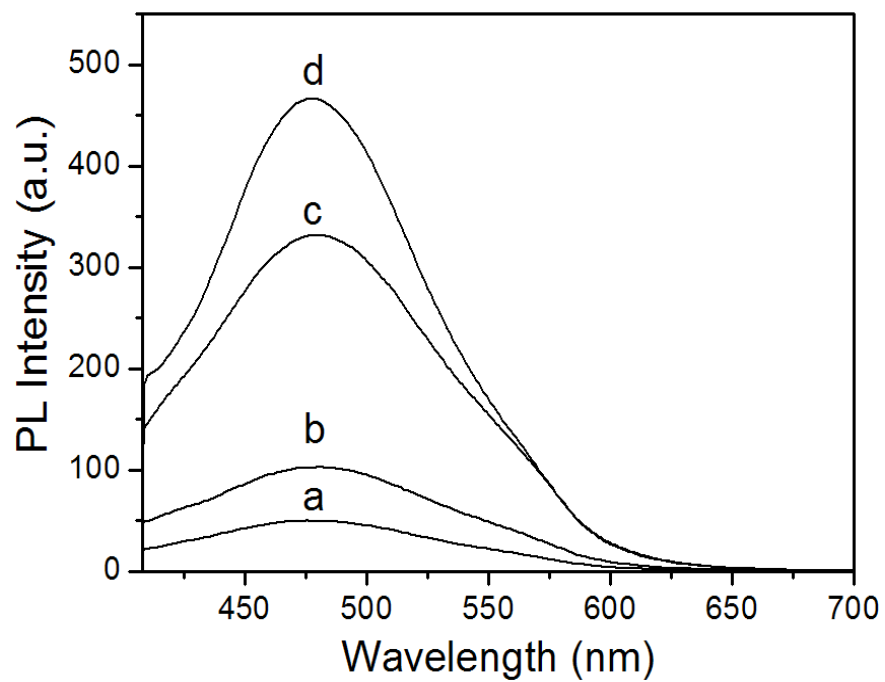


Fig. 4 The fluorescence spectra of ZnTe/ZnSe QDs with different ratios of Se-to-Te (a) 5:1 (b) 10:1 (c) 30:1 (d) 20:1.

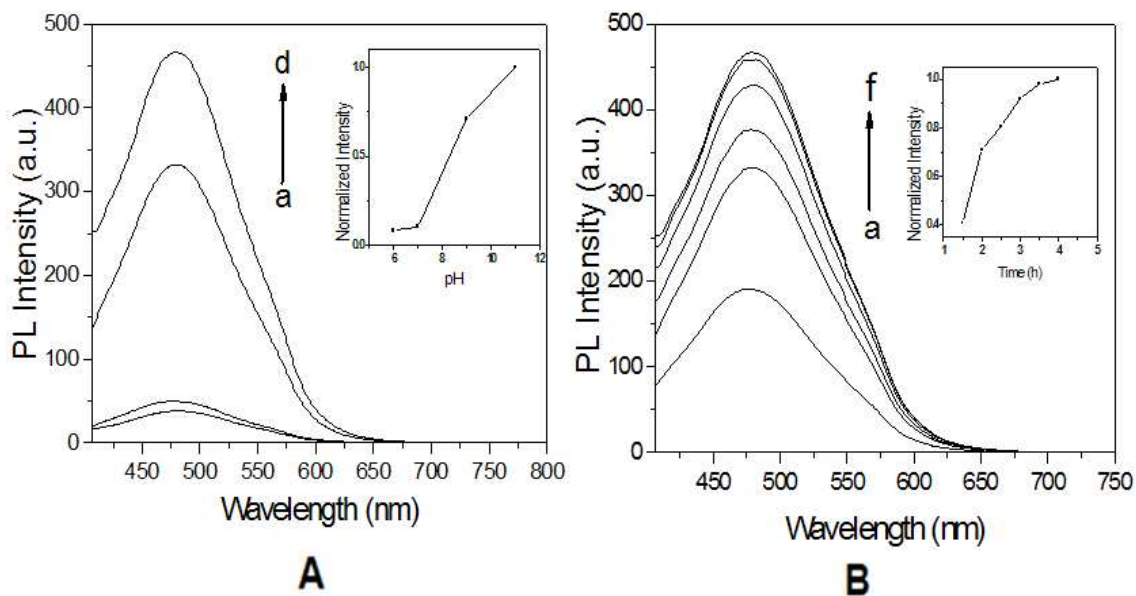


Fig. 5 (A) The influence of pH on the PL intensity of ZnTe/ZnSe QDs (a) pH 6 (b) pH 7 (c) pH 9 (d) pH 10. Inset: A plot of normalized intensity against the pH. (B) The influence of heating time on the PL intensity of ZnTe/ZnSe QDs (a) 1.5 h (b) 2 h (c) 2.5 h (d) 3 h (e) 3.5 h (f) 4 h. Inset: A plot of normalized intensity against the heating time.

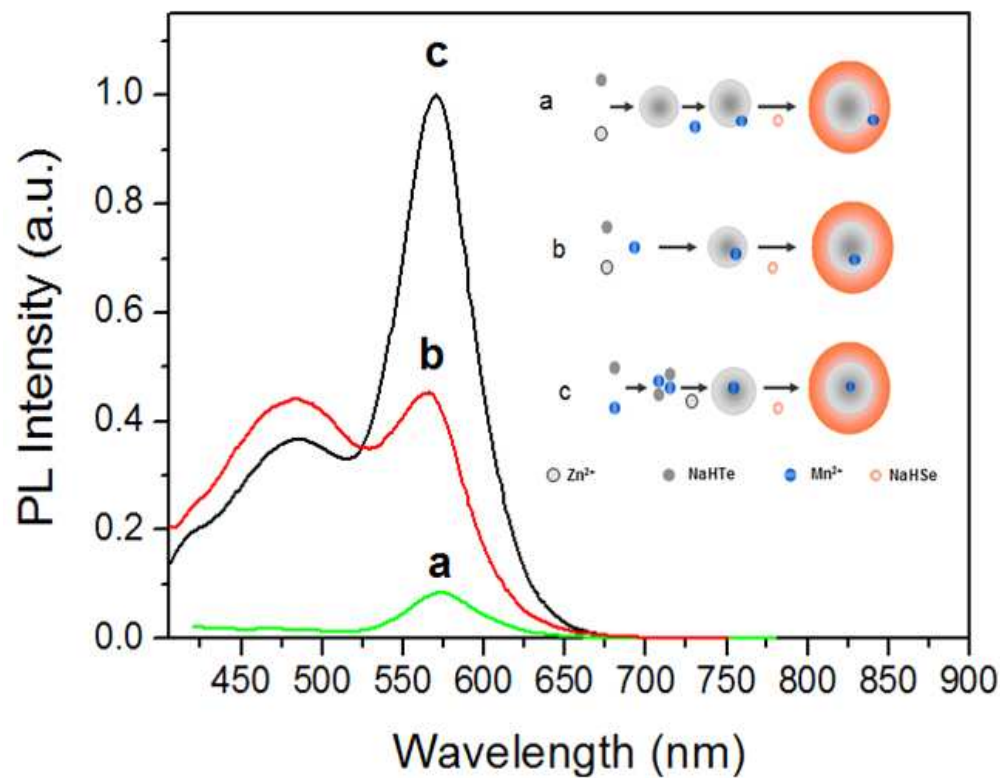


Fig. 6 The fluorescence spectra of Mn:ZnTe/ZnSe QDs with different synthesis methods (a) Dopant Mn²⁺ introduction after ZnTe nucleation (growth doping) (b) Dopant Mn²⁺ introduction along with host precursors Zn²⁺ and NaHTe (c) Dopant Mn²⁺ introduction before nucleation of ZnTe (nucleation doping). Inset: The schematic illustration of (a) (b) and (c)

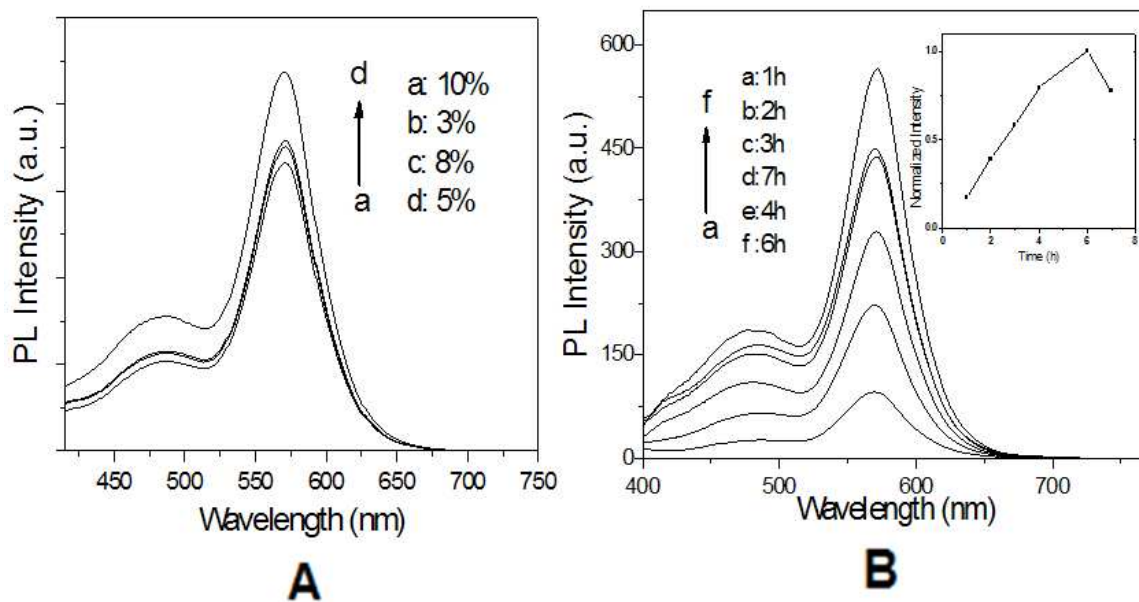


Fig. 7 The fluorescence spectra of ZnTe/ZnSe QDs with (A) different ratios of Mn-to-Zn (a) 10% (b) 3% (c) 8% (d) 5% and (B) different heating time (a) 1 h (b) 2 h (c) 3 h (d) 7 h (e) 4 h (f) 6 h.

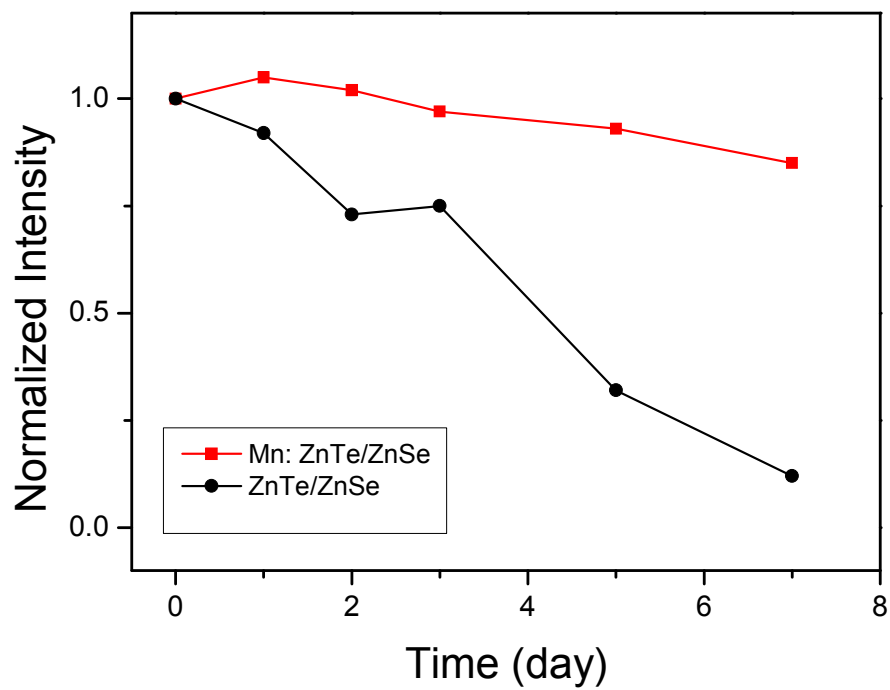


Fig. 8 Stability of ZnTe/ZnSe QDs and Mn: ZnTe/ZnSe QDs in daylight.

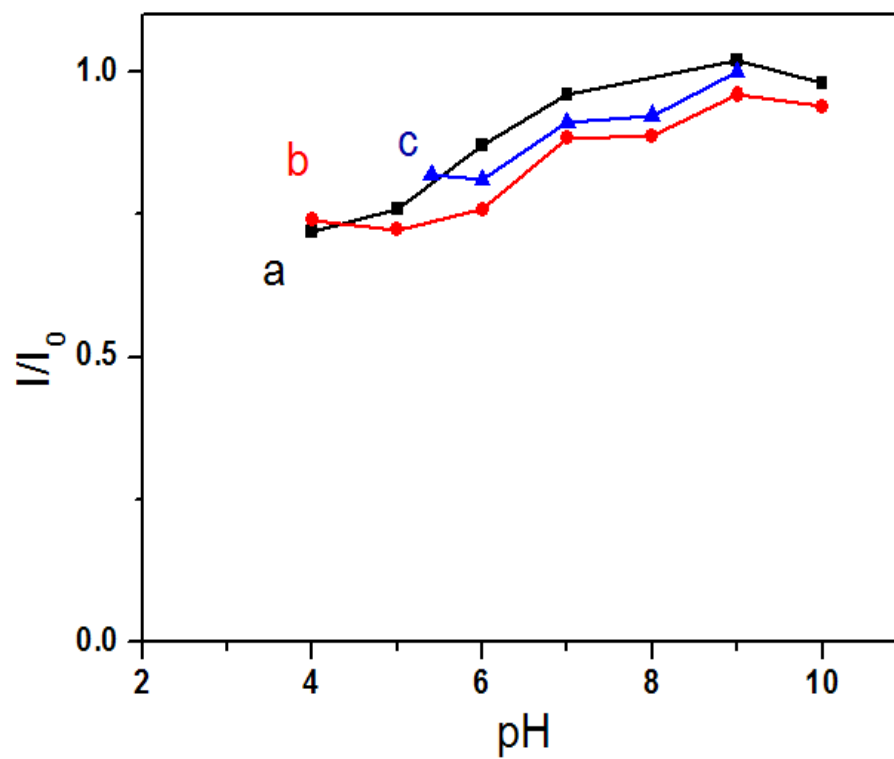


Fig. 9 Stability of Mn: ZnTe/ZnSe QDs in (a) phosphate, (b) TRIS and (c) borate buffered saline system.